Volume 21
Number 9
7 March 2025
Pages 1595–1772

Soft Matter

rsc.li/soft-matter-journal

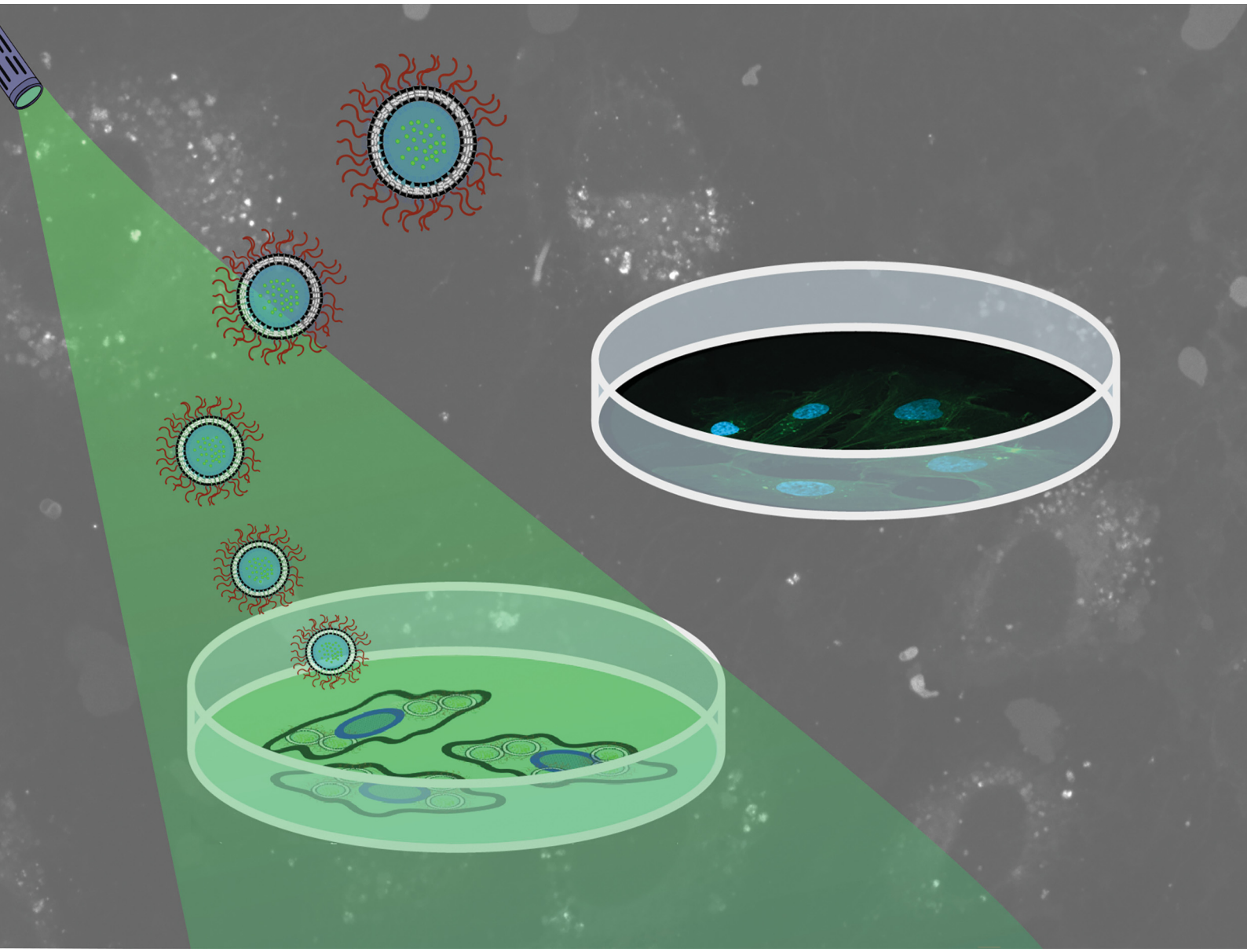

ISSN 1744-6848

ROYAL SOCIETY OF CHEMISTRY

PAPER
Bart Jan Ravoo *et al.*
Nanocarriers for intracellular delivery of molecular payloads triggered by visible light

20 YEARS ANNIVERSARY

Soft Matter

PAPER

View Article Online
View Journal | View Issue

Cite this: *Soft Matter*, 2025, **21**, 1639

Nanocarriers for intracellular delivery of molecular payloads triggered by visible light†

Ashutosh Kanojiya,[a] Julian Terglane,[b] Volker Gerke[bc] and Bart Jan Ravoo*[ac]

Received 22nd October 2024,
Accepted 10th December 2024

DOI: 10.1039/d4sm01239a

rsc.li/soft-matter-journal

Stimuli-responsive nanocontainers have emerged as promising vehicles to deliver molecular payloads into the cytosol of cells in a spatially, temporally and dosage-controlled manner. These nanocontainers respond to a specific type of stimulus such as a change in redox status, enzymatic activity, pH, heat, light, and others. In this work, we introduce photoresponsive nanocontainers based on the self-assembly of vesicles with surface-confined cyclodextrin–adamantane host–guest chemistry. The nanocontainer surface is protected by a polymer shell with a tetrazine cross-linker that enables triggered delivery of payloads upon exposure to green light (515 nm). We show that the release of vesicle-encapsulated payload is achieved also in cells by visible light, which is less harmful than the UV-light responsive release reported previously for *in vitro* systems.

Introduction

Nanocarriers have gained widespread attention in the field of molecular payload delivery especially for therapeutic uses. Stimuli responsive nanocarriers play an important role as they have been shown to overcome several challenges associated with the field, including but not limited to bioavailability, biocompatibility, non-specific delivery, toxicity, uncontrollable release and insufficient stability.[1–6] The versatile and multifunctional motifs introduced to confer stimuli responsiveness have shown promising results. They include methods such as targeted delivery by surface modification, polymer shells for longer retention times, endosomal escape of cargo upon photothermal heating, stimuli-response to specific target sites in the case of endogenous stimuli, and spatial-temporal control by exogeneous stimuli.[7–9] Some of the major stimuli that have been used are pH,[10,11] redox activity,[12,13] temperature,[14,15] light,[16–18] and magnetism;[19,20] multi-stimuli[21–23] responsive systems have also been developed. Light has been the stimulus that stands out as it is exogenous and can be applied with a high degree of spatio-temporal control. Light has major advantages such as less off-target effects and tuneable delivery according to the conditions required in the system.[8,24–27] Light responsive systems can be divided into those responding to UV (ultraviolet), visible and NIR (near infrared) light. However, whereas UV light can cause harm to living cells and organisms, visible light and NIR light are less harmful. Moreover, visible light and NIR light have the advantage of deeper penetration in organic matter as compared to UV light. There are several light-cleavable chemical linkers available, but most of them are responsive to harmful UV light, and there are only a few examples of visible light and NIR light responsive linkers.[28–30] Hence, there is a need to develop novel visible light responsive systems based on visible light responsive chemical linkers. Although visible light responsive nanocarriers have been reported for anticancer drug delivery by Singh and co-workers, and there are not many other examples of visible light responsive release using nanocarriers.[31] Here, we introduce a stable biocompatible visible light responsive system for intracellular delivery using self-assembled nanocontainers based on vesicles. These nanocontainers have been designed with the idea of meeting the challenges faced by drug delivery systems such as biocompatibility, controllable payload release, and minimal toxicity.

Results and discussion

Preparation and characterization of light-responsive nanocontainers

The cyclodextrin core of the light responsive nanocarrier is inspired by our previously reported supramolecular system relying on polymer shelled vesicles. These vesicles were prepared from amphiphilic cyclodextrin *via* self-assembly.[32] Amphiphilic cyclodextrin was deposited as a thin film and water was added to form multilamellar vesicles that were extruded by using a 100 nm filter several times to regulate

[a] *Organic Chemistry Institute, University of Münster, Münster, Germany. E-mail: b.j.ravoo@uni-muenster.de*
[b] *ZMBE, Center for Molecular Biology of Inflammation, University of Münster, Münster, Germany*
[c] *Center for Soft Nanoscience, University of Münster, Münster, Germany*

† Electronic supplementary information (ESI) available: Materials and methods, synthesis and analysis, and additional experimental data. See DOI: https://doi.org/10.1039/d4sm01239a

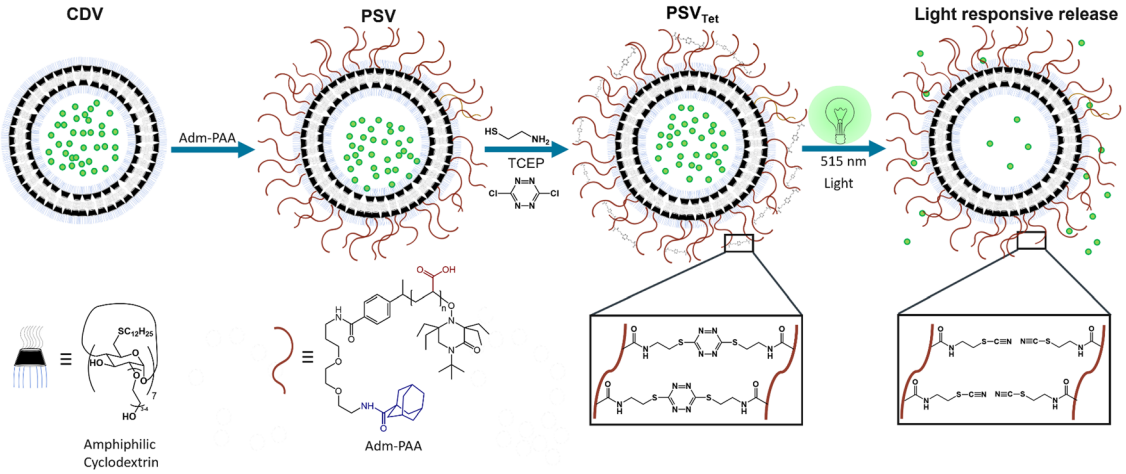

Fig. 1 Top: Schematic representation of the formation of visible light responsive nanocontainers and the release of molecular payloads in cells upon exposure to green light (λ = 515 nm). Bottom: Molecular structures and chemical reactions of essential components.

the size (further details can be found in the ESI†). As described, this allows subsequent host–guest chemistry for surface modification.[33] Applying adamantane linked polyacrylic acid (Adm-PAA) results in polymer decorated vesicles with a shell that reduces leaking of the molecular payload from the nanocontainer.[34–38] The polymer layer further provides a platform for crosslinking and thus control over the release of molecular payload from the system can be achieved. Previously, we developed this approach to produce redox responsive as well as enzyme responsive nanocontainers.[13,23] Now we have further enhanced our system towards the production of light responsive nanocontainers that can release the molecular payload by breaking the crosslinks under spatio-temporal control [Fig. 1].

The light responsive release was achieved with the help of a tetrazine based crosslinker. It is known that tetrazine dithioethers photodegrade upon visible light irradiation leading to relatively inert products.[39–41] 3,6-Dichloro-1,2,4,5-tetrazine has been used to crosslink thiol groups for various applications such as light responsive gelation and crosslinking peptides.[42–46] In our system, we first attached 2-aminoethane-1-thiol to various free acid groups on the surface of the vesicle by amide bonds resulting in free thiols. We then applied these free thiols in crosslinking reactions with 3,6-dichloro-1,2,4,5-tetrazine and thereby installed light responsive moieties on the surface of the nanocontainers.

Amphiphilic β-cyclodextrin self-assembles in the core structure of vesicles (CDV) as it is dispersed in water.[32] After this step, host–guest chemistry of the cyclodextrin and adamantane was used to cover the surface of the vesicles by adamantane linked polyacrylic acid (prepared according to the procedure in the ESI,† with a degree of polymerization of 340) and the structures thus formed are polymer shelled vesicles (PSV). The acid groups on the surface are further used to couple the 2-aminoethane-1-thiol *via* amide bond formation.[47] These thiols were then crosslinked in the last step with 3,6-dichloro-1,2,4,5-tetrazine to generate the crosslinked polymer shelled vesicles (PSV$_{Tet}$) [Fig. 1].

Next, we confirmed the formation of PSV$_{Tet}$ and characterized their properties. The self-assembly of the nanocontainers was tracked *via* dynamic light scattering (DLS). CDVs have a hydrodynamic diameter of 143 ± 3 nm, and after the addition of Ad-PAA polymer the outer shell is covered and hence an increase of the hydrodynamic diameter occurs, which is found to be at about 161 ± 8 nm. Finally, after crosslinking of the polymers, a further increase in size to 198 ± 11 nm is observed, which could be explained by some crosslinking between individual PSV$_{Tet}$ [Fig. 2a].[13] The molecular payload (FITC-phalloidin) containing PSV$_{Tet}$ were also characterized *via* DLS showing a hydrodynamic diameter of *ca.* 175 nm, similar to the empty PSV$_{Tet}$. This shows that encapsulation has no observable effect on the size of the nanocontainers [Fig. S6, ESI†]. To test the stability of the nanocontainers, we monitored the hydrodynamic diameter and PDI of PSV$_{Tet}$ over a course of 7 days. It was found that the hydrodynamic diameter remains in the range of 135–170 nm and PDI remains in the range of 0.13 to 0.18, which establishes that these nanocontainers are highly stable for a long period of time [Fig. S10, ESI†]. Also, PSV$_{Tet}$ were analyzed by using atomic force microscopy (AFM) and the size was found to be 144 ± 16 nm (n = 3) [Fig. 2b].

We further investigated the stepwise preparation of PSV$_{Tet}$ *via* zeta potential measurements. Over the course of our measurements, we observed that CDV exhibits the minimum charged state with a surface charge value of −7 mV. The negatively charged polymer (Adm-PAA) covering the surface of the CDV after introducing it *via* host–guest chemistry in the next step leads to a surface charge of −16.6 mV for PSV. In the final step amide bond formation takes place as 2-aminoethane-1-thiol is added and the zeta potential of PSV$_{Tet}$ increases due to reduction of the negative charge to a value −10 mV in accordance with the modifications applied [Fig. 2c]. The values of the DLS and zeta potential also correspond to the values that were achieved during the formation of other stimuli responsive vesicles with similar procedures.[13] Furthermore, infrared (IR) spectroscopy was performed. PSV SH (after addition of

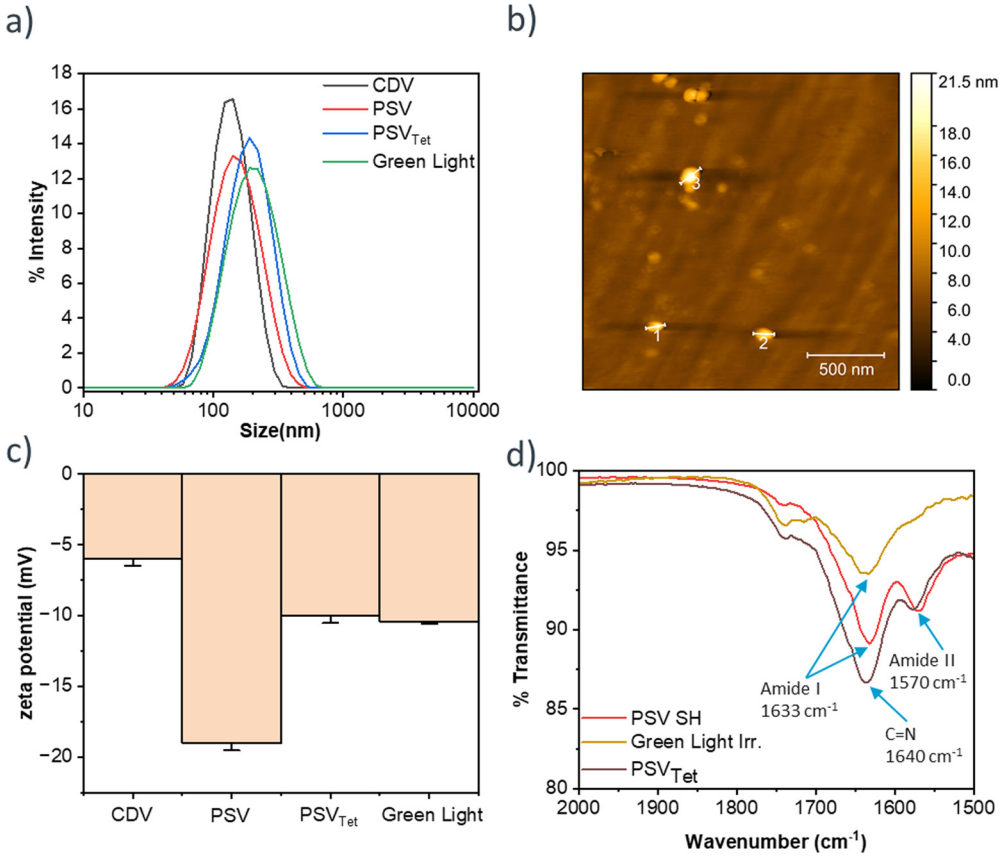

Fig. 2 Physico-chemical analysis of nanocontainers. (a) DLS. (b) AFM of only PSV_{Tet} with sections (1) 128 nm, (2) 144 nm, and (3) 160 nm. (c) ζ-Potential measurements of CDV, PSV, PSV_{Tet} and green light (515 nm, 3 W) irradiated PSV_{Tet}. Data represent mean ± standard deviation (n = 3). (d) IR measurements of PSV-SH (2-amine ethane-1-thiol linked PSV), PSV_{Tet} and green light (515 nm, 3 W) irradiated sample of PSV_{Tet}. Concentration of vesicles: 100 μM (CDV in HEPES buffer pH 7).

2-aminoethane-1-thiol to PSV) showed peaks at 1633 cm^{-1} and 1570 cm^{-1} that can be attributed to the amide group.[13] These peaks can also be observed in green light irradiated PSV_{Tet}. Freshly prepared non-irradiated PSV_{Tet} shows a peak at 1640 cm^{-1} that corresponds to C=N signifying the presence of crosslinked tetrazine [Fig. 2d].[42]

The nanocontainers were also examined by transmission electron microscopy (TEM) showing that PSV_{Tet} were of the size of 80–140 nm [Fig. S4, ESI†]. There is a decrease in the size with respect to DLS as expected since the nanocarriers are dehydrated during preparation of the TEM samples. Also, the nanocontainers were analysed after the release of the molecular payload upon green light treatment revealing a size similar to the non-irradiated specimen. This observation signifies that the basic structure of the nanocontainers is conserved and only the molecular payload is released *via* irradiation-mediated cleavage of crosslinks in the polymer shell [Fig. 2a].

Light responsive release from nanocontainers *in vitro*

In order to examine the light responsive release, PSV_{Tet} were prepared with pyranine dye as the molecular payload inside the nanocontainers. Pyranine is known as a water soluble, membrane impermeable fluorescent dye used for pH monitoring in cells.[48] This was used as the molecular payload in the nanocontainers as they could encapsulate water soluble species and fluorescence upon release could be tracked easily. The excess dye that was not encapsulated was removed *via* dialysis. Two samples of nanocontainers filled with pyranine were then exposed to green light (515 nm, 3 W, 2.8 mW cm^{-2}) and dark conditions, respectively. While the release of pyranine was observed using fluorescence spectroscopy for the duration of up to 8 h, it was observed that the nanocontainers exposed to green light released a higher amount of molecular payload as compared to the vesicles that were kept under dark conditions. We observed approximately 2.7× more release in the case of the green light irradiated sample in comparison to the sample kept in the dark after 8 h [Fig. 3a].

To confirm that the release is due to the light responsive crosslinker containing tetrazine, a non-responsive crosslinker (2,2′-(ethylenedioxy)bis(ethyleneamine)) was used to prepare the PSV_{Tet} and the release of the pyranine was monitored *via* fluorescence spectroscopy similar to the light responsive nanocontainers. No significant difference was observed in the amount of molecular payload released for irradiated and non-irradiated samples, confirming photodegradation of the crosslinker conferred responsiveness of the nanocontainers towards light [Fig. 3b]. To further validate the light responsive release, we performed an experiment where pyranine containing PSV_{Tet}

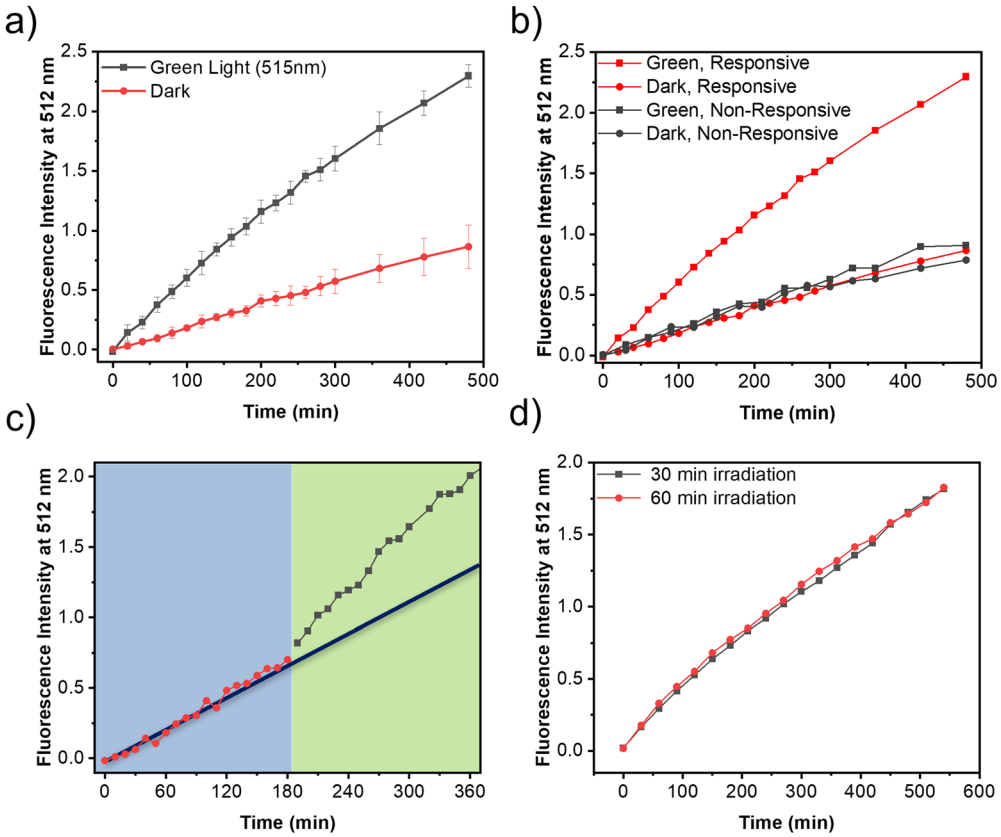

Fig. 3 Photo-responsive payload release from nanocontainers. (a) Release profile of pyranine from PSV_{Tet} in the dark and under green light irradiation. Data represent mean ± standard deviation (n = 3). (b) Release profile comparison of pyranine in the dark and under green light irradiation with visible light-responsive PSV_{Tet} and non-responsive PSV_{Tet}. (c) Release profile of pyranine from PSV_{Tet} kept in the dark for 180 min and then green light irradiated for a further 180 min. (d) Release profile of pyranine from PSV_{Tet} under green light irradiation with 30 min and 60 min irradiation times.

was first kept in the dark for 180 min and then exposed to green light for the next 360 min. We observed a significant change in the slope of the release of the molecular payload when the nanocontainers were exposed to green light, which corresponds to the faster release of the molecular payload. Together, this indicates that light is the cause of the enhanced release of the molecular payload from the nanocontainers [Fig. 3c].

To assess the influence of crosslinking on the release of the molecular payload (pyranine), we varied the amount of the crosslinker to 50% (300 μM) and 200% (600 μM) of the initial concentration used in the above experiments, respectively. In the case of the 50% crosslinker there is no significant difference in the release of molecular payload between the irradiated and non-irradiated samples [Fig. S2, ESI†]. In the case of the 200% crosslinker, the higher amount of crosslinker used resulted in the aggregation of nanocontainers as the hydrodynamic size increased from *ca.* 150 nm to *ca.* 640 nm and thus they could not be further utilized for delivery [Fig. S1, ESI†]. Hence the concentration of the crosslinker previously used were considered optimal for the release experiments (ESI†).

Furthermore, to investigate the crosslinking efficiency of PSV_{Tet}, 5-fluoresceinyl maleimide (5-FM) was used to trap the free thiols at various steps. 5-FM emits fluorescence upon binding to thiols at 518 nm. The fluorescence intensity was measured for PSV ET TCEP (PSV after adding 2-amino-ethane-1-thiol and TCEP), and PSV_{Tet} TCEP (PSV_{Tet} after adding TCEP). The difference between the fluorescence intensities at 518 nm indicates that the thiols were crosslinked *via* tetrazine with a crosslinking percentage estimated to be 15% (Fig. S5, ESI†).[16]

Uptake of nanocontainers and light responsive payload release in cells

After observing that the nanocontainers are capable of light responsive release *in vitro*, we were encouraged to test their performance in cells. Firstly, we wanted to establish the uptake of nanocontainers by cells. Therefore, we incubated human umbilical vein endothelial cells (HUVECs) with rhodamine-B labelled modified β-CDV.[49] The nanocontainers were incubated for 90 min with the cells and the samples were imaged *via* live cell imaging *via* confocal laser scanning microscopy (CLSM). Here, we could observe a strong colocalization of fluorescence signals of rhodamine B labelled nanocontainers (red) and a fluorescent endosomal marker (EGFP-Rab7, green) as quantified by Manders' coefficient. From this experiment we can conclude that the nanocontainers were taken up by the cells and at least to some extent were present in late endosomes following the conditions used for incubation [Fig. 4] (see Uptake in the ESI†).

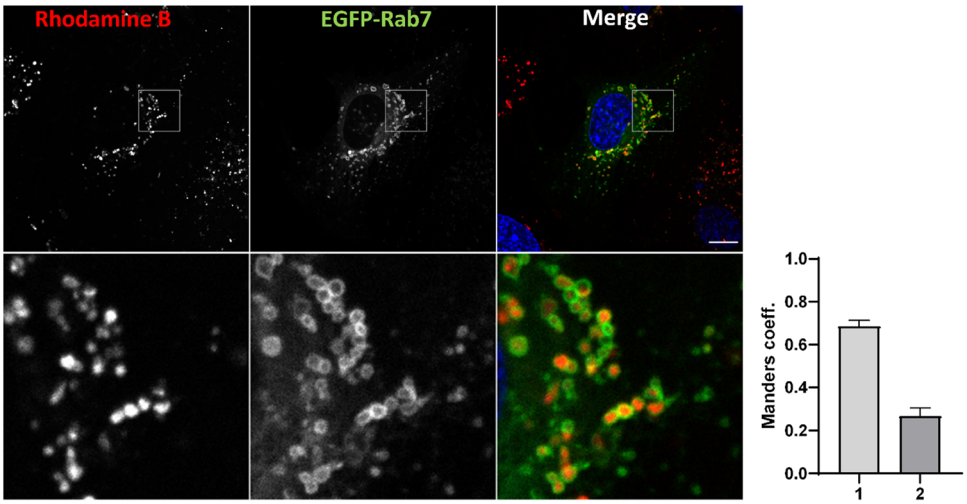

Fig. 4 Nanocontainers are endocytosed by HUVECs. Cells expressing EGFP-Rab7 as a marker for late endosomes were incubated with rhodamine B labelled light responsive containers. After an uptake of 90 min, cells were washed and incubated in medium for 2 h before being subjected to live cell imaging. Shown are the confocal microscope images of a single plane. The boxed area is enlarged below. DAPI staining of nuclei is shown in blue. Scale bar: 10 μm. The extent of colocalization of the fluorescence signals was quantified by determining Manders' coefficients. (1) Corresponds to the fraction of nanocontainer signal overlapping with the EGFP-Rab7 signal. (2) Corresponds to the fraction of EGFP-Rab7 signal overlapping with the nanocontainer signal. n = 20. Bars indicate the mean. Error bars show the SEM.

Next, we proceeded to test the light responsive delivery of the payload into the cytosol of cells. We first examined different irradiation times to initiate payload release. We performed the release experiment with 30 min and 60 min irradiation and observed no significant difference in the release of molecular payloads between these two experiments. We concluded that a 30 min irradiation time would be suitable to trigger release inside the cells [Fig. 3d] (Fig. S3, ESI†). Also, a phototoxicity assay was performed to assess whether the light irradiation might have any detrimental effects on HUVECs. It was observed that light irradiation (515 nm, 20 min) did not induce any significant effect on cell viability as compared to cells kept in the dark [Fig. S11, ESI†].

Nanocontainers were then prepared containing FITC-phalloidin as the molecular payload. Phallodin is a toxin that acts by strongly binding to F-actin in cells but is unable to cross the plasma membrane. Consequently, payload delivery is reflected by the extent of FITC-phalloidin staining of cytosolic

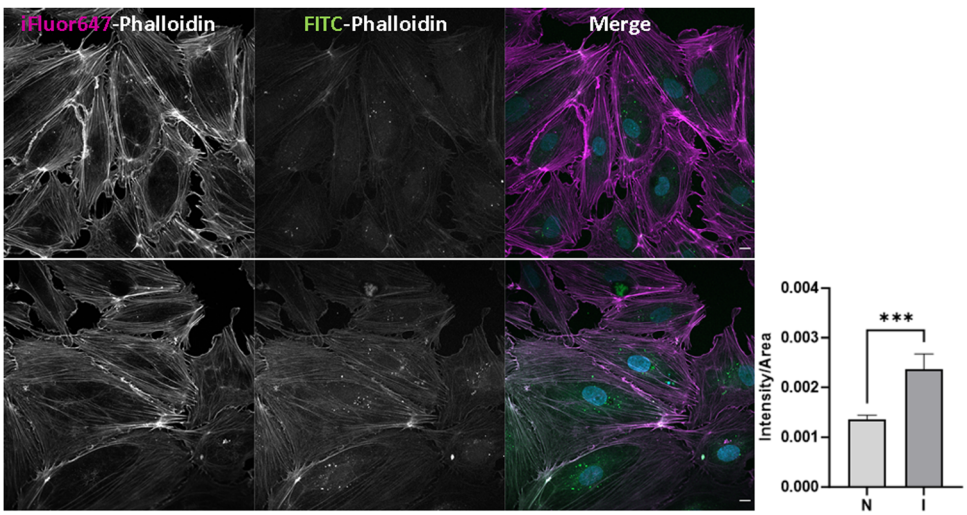

Fig. 5 Light-triggered release of FITC-phalloidin from endocytosed nanocontainers. HUVECs were treated with light responsive containers loaded with FITC-phalloidin according to the uptake protocol mentioned in the legend to Fig. 4 and subsequently either left untreated or irradiated with green light for 20 min. After 3 h cells were fixed with PFA and counterstained with phalloidin-iFluor647. Representative images of maximum intensity projections of z-stacks are shown for nonirradiated cells in the upper and for irradiated cells in the lower panels. Scale bars: 10 μm. The extent of cytosolic delivery of FITC-phalloidin was quantified by measuring the intensity of actin bound FITC-phalloidin and normalization to the area of identified actin structures (see Materials and methods, ESI†). n = 15. Bars indicate the mean. Error bars show SEM. Significance was obtained using a Mann–Whitney test. ****$p \leq 0.0001$, ***$p \leq 0.001$, **$p \leq 0.01$, *$p \leq 0.05$.

actin filaments.[50] FITC-phalloidin has also been introduced into cells with the help of nanocontainers before.[51] HUVECs were incubated with FITC-phalloidin loaded containers for 90 min and afterwards exposed to green light or kept in the dark for 20 min, respectively. We could observe that the cells that were exposed to green light showed 1.7× times higher fluorescence intensity per μm^2 as compared to the cells that were kept in the dark [Fig. 5]. Together, these findings suggest that following uptake into endosomes, the molecular payload of the novel nanocarriers can be released into the cytosol of cells (where the phalloidin can bind F-actin) following exposure to green light. Most likely, FITC-phalloidin is released into cytosol as the anionic polymer Adm-PAA can destabilize the endosomal membrane by affecting the membrane potential, which has been shown before to lead to the passive diffusion and release of FITC-phalloidin from endosomes.[23]

Conclusions

In this study we present a payload release system that enables intracellular delivery in response to visible light. This system is based on cyclodextrin vesicles templating a polymer shell on their surface *via* host–guest chemistry to suppress the leakage of molecular payload. The tetrazine linker equips the nanocontainers with light responsiveness. The use of light as a stimulus can help to achieve spatio-temporal control over the release of different molecular payloads. Pyranine as the molecular payload was released in *in vitro* experiments and FITC-phalloidin was introduced into cells *via* uptake of nanocarriers and subsequently released *via* irradiation with green light (515 nm), eliminating the need for harmful UV exposure.

Author contributions

BJR and AK conceptualised the work and improved it with the help of JT and VG. AK performed the synthesis, characterization and release experiments. JT performed the biological experiments along with AK. AK wrote the manuscript. JT reviewed and edited the manuscript. BJR and VG provided supervision and reviewed and edited the manuscript.

Data availability

The data supporting this article have been included as part of the ESI.†

Conflicts of interest

There are no conflicts to declare.

Acknowledgements

We are grateful to Lisa Schlichter for TEM measurements and Sarah Weischer for help with image analysis. AK and BJR would like to thank the CIM-IMPRS Graduate School at the University of Münster. This work was funded by the Deutsche Forschungsgemeinschaft (CRC 1459 Intelligent Matter – Project ID 433 682494).

Notes and references

1 S. Pottanam Chali and B. J. Ravoo, *Angew. Chem., Int. Ed.*, 2020, **59**, 2962–2972.
2 J. K. Patra, G. Das, L. F. Fraceto, E. V. R. Campos, M. D. P. Rodriguez-Torres, L. S. Acosta-Torres, L. A. Diaz-Torres, R. Grillo, M. K. Swamy, S. Sharma, S. Habtemariam and H.-S. Shin, *J. Nanobiotechnol.*, 2018, **16**, 71.
3 H. Jahangirian, E. G. Lemraski, T. J. Webster, R. Rafiee-Moghaddam and Y. Abdollahi, *Int. J. Nanomed.*, 2017, **12**, 2957–2978.
4 M. Fatima, W. H. Almalki, T. Khan, A. Sahebkar and P. Kesharwani, *Adv. Mater.*, 2024, **36**, 2312939.
5 F. Schibilla, A. Holthenrich, B. Song, A. L. Linard Matos, D. Grill, D. Rota Martir, V. Gerke, E. Zysman-Colman and B. J. Ravoo, *Chem. Sci.*, 2018, **9**, 7822–7828.
6 L. M. Randolph, M.-P. Chien and N. C. Gianneschi, *Chem. Sci.*, 2012, **3**, 1363–1380.
7 V. P. Torchilin, *Nat. Rev. Drug Discovery*, 2014, **13**, 813–827.
8 S. Mura, J. Nicolas and P. Couvreur, *Nat. Mater.*, 2013, **12**, 991–1003.
9 N. Brkovic, L. Zhang, J. N. Peters, S. Kleine-Doepke, W. J. Parak and D. Zhu, *Small*, 2020, **16**, 2003639.
10 E. Jäger, P. Černoch, M. Vragovic, L. J. Calumby Albuquerque, V. Sincari, T. Heizer, A. Jäger, J. Kučka, O. Š. Janoušková, E. Pavlova, L. Šefc and F. C. Giacomelli, *Biomacromolecules*, 2024, **25**, 4192–4202.
11 Y. Chen, H. Han, H. Tong, T. Chen, H. Wang, J. Ji and Q. Jin, *ACS Appl. Mater. Interfaces*, 2016, **8**, 21185–21192.
12 Z. Zhang, X. Xu, J. Du, X. Chen, Y. Xue, J. Zhang, X. Yang, X. Chen, J. Xie and S. Ju, *Nat. Commun.*, 2024, **15**, 1118.
13 W. C. de Vries, D. Grill, M. Tesch, A. Ricker, H. Nüsse, J. Klingauf, A. Studer, V. Gerke and B. J. Ravoo, *Angew. Chem., Int. Ed.*, 2017, **56**, 9603–9607.
14 K. Cai, F. Jiang, Z. Luo and X. Chen, *Adv. Eng. Mater.*, 2010, **12**, B565–B570.
15 V. Kozlovskaya, F. Liu, Y. Yang, K. Ingle, S. Qian, G. V. Halade, V. S. Urban and E. Kharlampieva, *Biomacromolecules*, 2019, **20**, 3989–4000.
16 Y. Wang, Y. Deng, H. Luo, A. Zhu, H. Ke, H. Yang and H. Chen, *ACS Nano*, 2017, **11**, 12134–12144.
17 H. Kang, A. C. Trondoli, G. Zhu, Y. Chen, Y.-J. Chang, H. Liu, Y.-F. Huang, X. Zhang and W. Tan, *ACS Nano*, 2011, **5**, 5094–5099.
18 H. Xiong, X. Li, P. Kang, J. Perish, F. Neuhaus, J. E. Ploski, S. Kroener, M. O. Ogunyankin, J. E. Shin, J. A. Zasadzinski, H. Wang, P. A. Slesinger, A. Zumbuehl and Z. Qin, *Angew. Chem., Int. Ed.*, 2020, **59**, 8608–8615.

19 J. Chen, T. Ren, L. Xie, H. Hu, X. Li, M. Maitusong, X. Zhou, W. Hu, D. Xu, Y. Qian, S. Cheng, K. Yu, J. A. Wang and X. Liu, *Nat. Commun.*, 2024, **15**, 557.
20 Y. Gao, M.-W. Chang, Z. Ahmad and J.-S. Li, *RSC Adv.*, 2016, **6**, 88157–88167.
21 F. Badparvar, A. P. Marjani, R. Salehi and F. Ramezani, *Sci. Rep.*, 2024, **14**, 8567.
22 F. Huang, W.-C. Liao, Y. S. Sohn, R. Nechushtai, C.-H. Lu and I. Willner, *J. Am. Chem. Soc.*, 2016, **138**, 8936–8945.
23 S. Kudruk, S. Pottanam Chali, A. L. Linard Matos, C. Bourque, C. Dunker, C. Gatsogiannis, B. J. Ravoo and V. Gerke, *Adv. Sci.*, 2021, **8**, 2100694.
24 Y. Tao, H. F. Chan, B. Shi, M. Li and K. W. Leong, *Adv. Funct. Mater.*, 2020, **30**, 2005029.
25 C. S. Sia, B. T. Tey and L. E. Low, *Adv. Funct. Mater.*, 2024, **34**, 2314278.
26 W. Zhao, Y. Zhao, Q. Wang, T. Liu, J. Sun and R. Zhang, *Small*, 2019, **15**, 1903060.
27 Y. Wang and D. S. Kohane, *Nat. Rev. Mater.*, 2017, **2**, 17020.
28 Y. Xue, H. Bai, B. Peng, B. Fang, J. Baell, L. Li, W. Huang and N. H. Voelcker, *Chem. Soc. Rev.*, 2021, **50**, 4872–4931.
29 Z. Wang, W. Bao, B. Wujieti, M. Liu, X. Li, Z. Ma, W. Cui and Z. Tian, *Angew. Chem., Int. Ed.*, 2024, e202413633.
30 H. Masai, T. Nakagawa and J. Terao, *Polym. J.*, 2024, **56**, 297–307.
31 S. Ray, S. Banerjee, A. K. Singh, M. Ojha, A. Mondal and N. D. P. Singh, *ACS Appl. Nano Mater.*, 2022, **5**, 7512–7520.
32 B. J. Ravoo and R. Darcy, *Angew. Chem., Int. Ed.*, 2000, **39**, 4324–4326.
33 P. Falvey, C. W. Lim, R. Darcy, T. Revermann, U. Karst, M. Giesbers, A. T. M. Marcelis, A. Lazar, A. W. Coleman, D. N. Reinhoudt and B. J. Ravoo, *Chem. – Eur. J.*, 2005, **11**, 1171–1180.
34 W. C. de Vries, M. Niehues, M. Wissing, T. Würthwein, F. Mäsing, C. Fallnich, A. Studer and B. J. Ravoo, *Nanoscale*, 2019, **11**, 9384–9391.
35 W. C. de Vries, M. Tesch, A. Studer and B. J. Ravoo, *ACS Appl. Mater. Interfaces*, 2017, **9**, 41760–41766.
36 Y. Lu, W. C. de Vries, N. J. Overeem, X. Duan, H. Zhang, H. Zhang, W. Pang, B. J. Ravoo and J. Huskens, *Angew. Chem., Int. Ed.*, 2019, **58**, 159–163.
37 A. Samanta, M. Tesch, U. Keller, J. Klingauf, A. Studer and B. J. Ravoo, *J. Am. Chem. Soc.*, 2015, **137**, 1967–1971.
38 S. Himmelein, V. Lewe, M. C. A. Stuart and B. J. Ravoo, *Chem. Sci.*, 2014, **5**, 1054–1058.
39 D. S. King, C. T. Denny, R. M. Hochstrasser and A. B. Smith, III, *J. Am. Chem. Soc.*, 1977, **99**, 271–273.
40 D. Coulter, D. Dows, H. Reisler and C. Wittig, *Chem. Phys.*, 1978, **32**, 429–435.
41 J. H. Glownia and S. J. Riley, *Chem. Phys. Lett.*, 1980, **71**, 429–435.
42 C. Wang, C. Liu, Q. Wei, L. Yang, P. Yang, Y. Li and Y. Cheng, *Research*, 2020, 6563091.
43 D. S. Rivero, R. E. Paiva-Feener, T. Santos, E. Martín-Encinas and R. Carrillo, *Macromolecules*, 2021, **54**, 10428–10434.
44 G. Clavier and P. Audebert, *Chem. Rev.*, 2010, **110**, 3299–3314.
45 A. Borges, C. Nguyen, M. Letendre, I. Onasenko, R. Kandler, N. K. Nguyen, J. Chen, T. Allakhverdova, E. Atkinson, B. DiChiara, C. Wang, N. Petler, H. Patel, D. Nanavati, S. Das and A. Nag, *ChemBioChem*, 2023, **24**, e202200590.
46 M. J. Tucker, J. R. Courter, J. Chen, O. Atasoylu, A. B. Smith Iii and R. M. Hochstrasser, *Angew. Chem., Int. Ed.*, 2010, **49**, 3612–3616.
47 A. Blasi-Romero, C. Palo-Nieto, C. Sandström, J. Lindh, M. Strømme and N. Ferraz, *Polymers*, 2021, **13**, 249.
48 Y. Avnir and Y. Barenholz, *Anal. Biochem.*, 2005, **347**, 34–41.
49 J. Voskuhl, T. Fenske, M. C. A. Stuart, B. Wibbeling, C. Schmuck and B. J. Ravoo, *Chem. – Eur. J.*, 2010, **16**, 8300–8306.
50 M. An, D. Wijesinghe, O. A. Andreev, Y. K. Reshetnyak and D. M. Engelman, *Proc. Natl. Acad. Sci. U. S. A.*, 2010, **107**, 20246–20250.
51 K. Dhakal, B. Black and S. Mohanty, *Sci. Rep.*, 2014, **4**, 6553.